Presented at the 23rd European Photovoltaic Solar Energy Conference, Valencia, Spain, 1-5 September 2008

MULTI-JUNCTION POLYMER SOLAR CELLS

W. Eerenstein, L.H. Slooff, S. Böhme, E. Voroshazi, S.C. Veenstra, J.M. Kroon
ECN Solar Energy, PO Box 1, 1755 ZG Petten, The Netherlands

ABSTRACT: We discuss the materials challenges for increasing cell efficiencies of polymer solar cells via the route of stacking several cells on top of each other in multi-junction solar cells. For such cells, the recombination layer between the two sub cells is crucial. Typically, the recombination layer consists of a semi-transparent n- and p-type semiconductor bilayer. Several options for the recombination layer will be discussed. Furthermore, we discuss how the workfunction and the conductivity of the semi-transparent semiconductors may influence the performance of the cells. We also discuss requirements for accurate measurements of spectral response and efficiency.
Keywords: tandem, polymer film, multi-junction solar cell

1 INTRODUCTION

Polymer based solar cells offer the possibility of low cost solution processing. A blend solution containing the light absorbing polymer and an electron acceptor (fullerene derivatives, e.g. PCBM) offer the possibility for printing, spray coating or doctor blade type processing. Although large improvements have been made recently, the efficiency and stability of these solar cells are presently insufficient for large scale applications. The record independently verified efficiency is 5.4 % [1]. An important reason for the relatively low efficiency is the fact that many conducting polymers applied in solar cells have a band gap around 2 eV. Consequently, a large part of the solar spectrum is not absorbed by the polymer. A second reason is the low charge carrier mobility in polymers, which limits the thickness of these cells to several hundreds of nanometers. As a result of this thickness, the polymer films are still semi-transparent.
One strategy to improve the efficiency of polymer based solar cells is the application of low band gap polymers [2]. These polymers absorb a larger fraction of the solar spectrum which allows for higher photocurrent densities in photovoltaic devices. However, the band gap can also influence the open circuit voltage (V_{oc}) of the photovoltaic device. It is anticipated that the optimum band gap for a polymer solar cell (with a single photoactive layer) is between 1.4 and 2.0 eV. [3,4]. Over the last five years, many low band gap polymers have been synthesized, see e.g. [2,5,6].
The availability of low bandgap polymers opens another route to increase the efficiency of polymer solar cells, namely by stacking two – or more – polymer cells with different optical band gaps on top of each other in so called multi-junction solar cells. Fig. 1 shows a schematic drawing of a monolithic, two terminal tandem solar cell. In such a multi-junction solar cell, the subcells need to be separated from each other by a recombination layer.
For higher cell efficiencies, yet maintaining the option of low cost processing, there are several requirements for both the polymer materials and for the recombination layer. The optical bandgap of the polymer should be tuned below 1.5 eV, e.g. through changing the polymer backbone. Care has to be taken that the polymer and fullerene are still soluble and processable. When the bandgap is reduced, this might result in a lower V_{oc}. Higher efficiencies are then only obtained when the current density overcompensates the loss in V_{oc}. The most successful low bandgap polymers to date possess a bandgap of 1.4 eV [2,5,6].

Besides demands for the polymer materials employed, the recombination layer between the two cells also has several requirements: 1) optically transparent, 2) inert to the bottom solar cell, 3) protect the bottom solar cell when processing the top cell, 4) in order to keep processing costs down, it must be possible to apply this layer by solution processing. This set of requirements severely limits the number of possible materials.
For the recombination layer, two solution processable options have been identified and fabricated. One is a combination of a thin ZnO layer processed directly on the bottom cell and a pH neutral PEDOT:PSS layer processed on top of the ZnO [7]. As ZnO dissolves in acids, standard PEDOT:PSS (pH~2) can not be processed on top and pH neutral PEDOT is necessary. Another possibility is a thin TiOx layer processed from a precursor solution [8]. TiOx does not dissolve in acids and normal PEDOT can be processed on top of it.

A multi-junction with both options is schematically shown in Fig. 1.

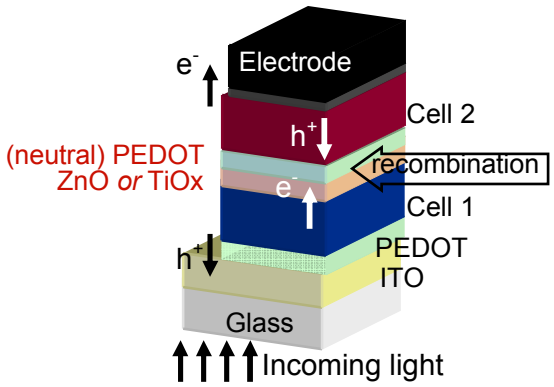

Figure 1: Schematic drawing of a monolithic polymer multi-junction cell with recombination layer consisting of either ZnO/pH neutral PEDOT, or TiOx/PEDOT.

In such a multi-junction configuration the two cells are electrically connected in series by the recombination layer. The total voltage is then the sum of the voltage of the individual cells, and the total current density is determined by the cell with the lowest current density. In order to obtain high efficiency, it is thus necessary to optimize and match the currents in both cells. This optimisation process is aided by optical modeling, where the current density in both cells can be calculated as a function of film thickness [9,10].

Apart from the fabrication issues raised above, there is the issue of characterization. Both for single junction and for multi-junction devices, correct measurements will depend on the active area and geometry and an optical mask might be required. Determining the efficiency of multi-junction cells correctly is not trivial, and the spectral response measurements must be performed with appropriate bias light and bias voltage. In this paper, we will discuss the synthesis and characterization of the recombination layer and cell performance, as well as the requirements for characterization of single- and multi-junction polymer solar cells.

2 EXPERIMENTAL

Single cells have been processed in the following way. An indium tin oxide (ITO) coated glass substrate was first thoroughly cleaned and subsequently a PEDOT:PSS (Baytron/Clevios P AI4083 from HC Starck, referred to as PEDOT) layer was spincoated on top. Polymer blend layers of either poly(9,9-didecanefluorene-alt-(bisthienylene) benzothiadiazole) (PF10TBT), poly3-hexyl thiphene (P3HT) or poly[2-methoxy-5-(3',7'-dimethyloctyloxyl)]-1,4-phenylene vinylene (MDMO-PPV) mixed with [6,6]-phenyl C_{61}-butyric acid methyl ester (PCBM, Solenne BV) have been employed by spincoating from:

- a 0.5 wt.% PF10TBT:PCBM (1:4) solution in chlorobenzene (CB) stirred overnight at 70 °C
- 0.75 wt.% MDMO-PPV:PCBM (1:4) solution in CB stirred overnight at 75 °C
- 1.28wt.% P3HT:PCBM (1:1) solution in CB stirred overnight at 70 °C

The LiF/Al and LiF/Al/Au contacts were thermally evaporated. Single cells of PF10TBT and MDMO-PPV have also been fabricated with a pH neutral layer of PEDOT (Orgacon, batch 5541073, pH=7, 1.2 wt %, Agfa Gevaert NV, a kind gift of the Technical University of Eindhoven). The spincoating conditions were the same as for devices made with standard PEDOT.

Two types of tandem cells have been fabricated. One was a mechanical stack of two single junction polymer: fullerene cells [11]. The bottom cell consists of a blend of PF10TBT:PCBM and the top cell is a MDMO-PPV:PCBM blend (the top cell is the cell that receives light first). The electrical contact on the MDMO-PPV:PCBM layer consisted of LiF(1nm)/Al(2.5 nm)/Au(12.5 nm) and was semitransparent. The complete device structure is given in Fig. 2.

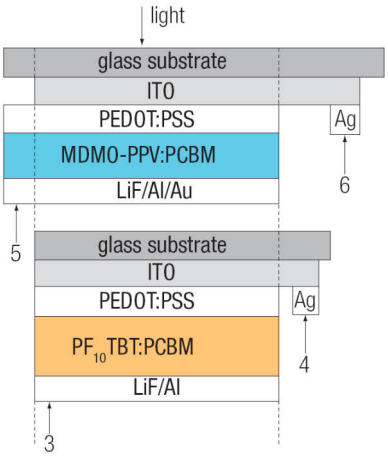

Figure 2: Schematic drawing of a mechanically stacked polymer based multi-junction cell. The individual polymer cells of MDMO-PPV:PCBM and PF10TBT:PCBM can be measured separately (contact 5&6 and 3&4) and the whole stack can be measured in a series connection (contacts 3&6).

Integrated tandem cells with a geometry as shown in Fig. 1 have been made by subsequently depositing standard PEDOT, PF10TBT:PCBM, ZnO, pH neutral PEDOT and PF10TBT:PCBM, or by applying MDMO-PPV:PCBM and PF10TBT:PCBM as the active layers. Thicknesses of the active layers were approximately 150 nm and 100 nm for the top and bottom layers respectively. All layers have been deposited by spincoating as described above. LiF/Al contacts were thermally evaporated on top. The ZnO nanoparticle dispersion was synthesised via a Zn acetate / KOH solution in methanol [7].

Current-voltage (I/V) measurements were done in a setup containing a Keithley 2400 SourceMeter wired to a sample holder in a nitrogen-filled glove box. The sample was illuminated by a halogen lamp. An automated rotating filter wheel was used to record the current densities at various wavelengths for external quantum efficiency (EQE) measurement. Measurements have been performed with and without an optical mask. For multijunction devices, bias light was applied either via a LED ring with 20 LEDs or via a halogen lamp with a band pass filter. A silicon reference cell with known spectral response was used for calibration purposes, enabling the calculation of the estimated AM1.5 short circuit current density.

3 RESULTS AND DISCUSSION

3.1 Single cells with ZnO and pH neutral PEDOT

ZnO layers have been processed on glass substrates to study the thickness and quality of those layers. Fig. 3 shows a SEM image of a 50 nm thick ZnO film processed by spincoating from a ZnO nanoparticle dispersion.

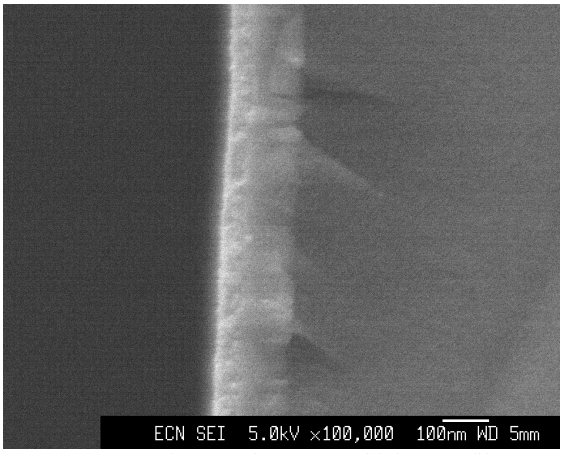

Figure 3: SEM image of a 50 nm thick ZnO film on a glass substrate. From right to left, the glass substrate, the ZnO layer (110 nm) shows a flat interface with the glass and a smooth surface.

In order to verify whether the presence of ZnO on top of the polymer blend layer influences the performance of the cell, we have fabricated single cells of PF10TBT:PCBM with a thin (30 nm) ZnO layer on top. Optical modeling has shown that the presence of ZnO can influence the amount of light absorbed in the polymer layer, and thus the current density, by a maximum of 10% as described in [10]. The V_{oc} and FF should not be influenced. For a 180 nm thick PF10TBT:PCBM cell the I/V curve with and without ZnO is shown in Fig. 4. Indeed, the current density, V_{oc} and FF are very similar for both cells.

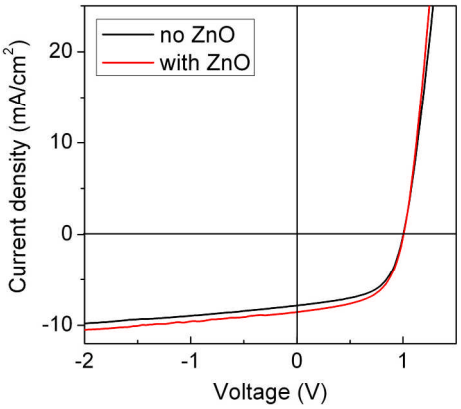

Figure 4: I/V curve of a 180 nm thick PF10TBT:PCBM cell with and without a 30 nm ZnO layer on top.

The influence of pH-neutral PEDOT on the V_{oc} has been studied for single cells with PF10TBT:PCBM, MDMO-PPV:PCBM and P3HT:PCBM and is shown in Fig. 5. For PF10TBT:PCBM devices, pH-neutral PEDOT has a large influence on the V_{oc}, which drops from 1 V for standard PEDOT:PSS to 0.70 V for pH-neutral PEDOT as shown in Fig. 5a. For MDMO-PPV:PCBM devices the effect is less pronounced, with a drop from 0.84 to 0.70 V, shown in Fig. 5b. For P3HT:PCBM devices a small drop from 0.59 to 0.56 V was observed, see Fig. 5c. This effect on V_{oc} is related to the electronic levels of pH-neutral PEDOT [12], as shown in Fig. 6.

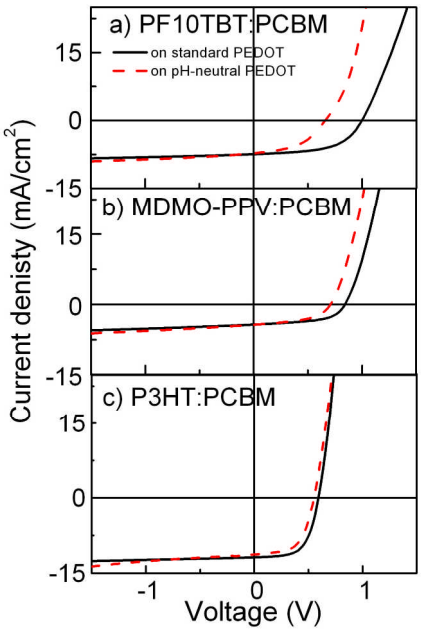

Figure 5: I/V curves of a) PF10TBT:PCBM cells on standard and on pH neutral PEDOT, resulting in a V_{oc} of 1 V and 0.70 V respectively and of b) MDMO-PPV:PCBM cells on standard and on pH neutral PEDOT, resulting in a V_{oc} of 0.84 V and 0.70 V respectively and of c) P3HT:PCBM cells standard and on pH neutral PEDOT, resulting in a V_{oc} of 0.59 V and 0.56 V respectively.

The open-circuit voltage is proportional to the energy level difference between the acceptor's LUMO and the donor's HOMO. When the HOMO level of the donor material is below the HOMO level of the PEDOT, the V_{oc} is determined by the energy level difference between the PEDOT and acceptor's LUMO. For standard PEDOT, this means that the maximum open-circuit voltage is 1.1 ± 0.1eV and for the neutral PEDOT this becomes 0.7 ± 0.1eV. Devices fabricated with MDMO-PPV and PF10TBT on neutral PEDOT indeed show a V_{oc} of 0.7 V. The HOMO level of P3HT is closer to the HOMO level of neutral PEDOT and for P3HT devices, the observed difference in V_{oc} for standard and neutral PEDOT is indeed minor (0.59 and 0.56 V respectively).

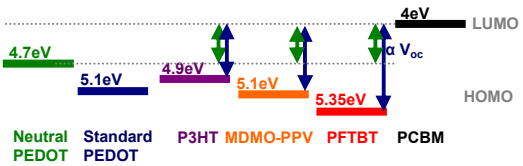

Figure 6: Energy levels of the neutral and standard PEDOT, as well as of PCBM and the investigated polymers.

3.2 Tandems

I/V curves of tandems cells consisting of PF10TBT as the active layers and tandems consisting of MDMO-PPV:PCBM and PF10TBT:PCBM as the active layers are shown in Fig. 7. The measured V_{oc} of the tandem cells is 1.68 V for the tandem consisting of the two PF10TBT:PCBM layers and 1.54 V for the tandem consisting of a MDMO-PPV layer and a PF10TBT:PCBM layer. These V_{oc} values are the sum of

the V_{oc} values of the individual sub cells, i.e. 0.85 V + 0.70 V for the PF10TBT layers on standard and on pH neutral PEDOT:PSS respectively and 0.84 V + 0.7 V for the MDMO-PPV layer on standard PEDOT and PF10TBT on pH neutral PEDOT. The measured current density for the tandem consisting of two PF10TBT layers is 4.6 mA/cm^2 measured under a halogen lamp (MPP = 2.8 mW/cm^2), resulting in an estimated AM1.5 current density of 3.7 mA/cm^2 (estimate based on the mismatch for a single junction PF10TBT cell). For the thickness combination of 100 nm/150 nm for the front and back cell this value corresponds to a calculated value of 3.8 mA/cm^2 [10]. If the voltage drop of 0.3 V resulting from the application of pH-neutral PEDOT could be prevented, a significant increase in the MPP could be achieved.

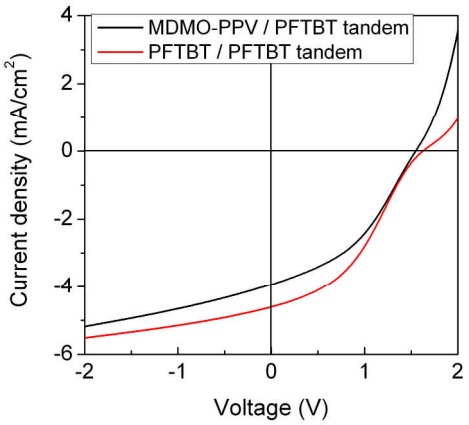

Figure 7: I/V curves of a MDMO-PPV:PCBM/PF10TBT:PCBM tandem cell and a PF10TBT:PCBM/PF10TBT:PCBM tandem cell.

3.3 TiOx

The voltage drop does not occur when normal PEDOT is employed. In that case, ZnO is not suitable as it dissolves when the acidic solutions are spincoated on top. A promising candidate to replace ZnO is TiOx [8]. TiOx can be processed from nanoparticle dispersions or from titanium isopropoxide precursor solutions. In the latter case, the precursor reacts with water from the air. To prevent rapid hydrolysis (which leads to non uniform layers), stabilizers such as ethanolamine and 2-methoxyethanol are added [8].

Attempts to reproduce this method have so far been unsuccessful. Although SEM images showed flat, closed layers and the optical transparency in the visible range is equal to the transparency of the glass substrate, single junctions with TiOx between the PF10TBT:PCBM and the counter electrode showed a strongly reduced current by a factor of 2.5 as shown in Fig. 8.

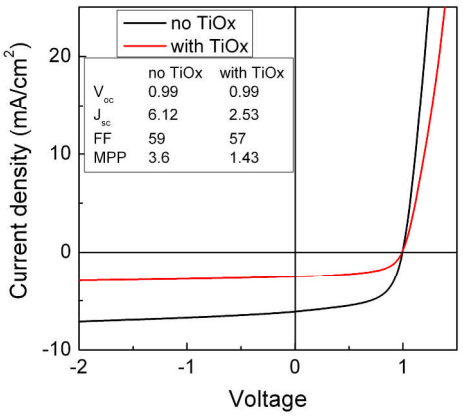

Figure 8: I/V curve of a 180 nm thick PF10TBT:PCBM cell with and without a 30 nm TiOx layer on top.

The reduced current indicates that the TiOx acts as a blocking layer. Partial hydrolysis of the titanium isopropoxide precursor, a different workfunction or the thickness of the layer could be responsible. This is subject to further investigation. Tandem structures with TiOx/PEDOT:PSS have not been synthesized successfully, as the deposition of PEDOT:PSS on top of TiOx resulted in rough, uneven surfaces.

3.4 Measurement of solar cells

3.4.1 Influence of cell area

The influence of device layout on the performance of polymer solar cells and the importance of using an illumination mask in case of a crossed layout have been studied by [13,14]. Charges generated close to the active area can still be collected, particularly when neutral PEDOT is employed due to its relatively high conductivity. The active areas of the solar cells are 0.093 cm^2, 0.164 cm^2, 0.364 cm^2 or 1.003 cm^2 and the corresponding mask sizes are 0.04 cm^2, 0.09 cm^2, 0.25 cm^2 and 0.8 cm^2.

The active area is determined by the overlapping regions of the patterned ITO and Al. Besides the active area we distinguish Region I: the active layer/PEDOT:PSS/ITO and Region II: Al/active area/PEDOT:PSS as represented in Fig. 9.

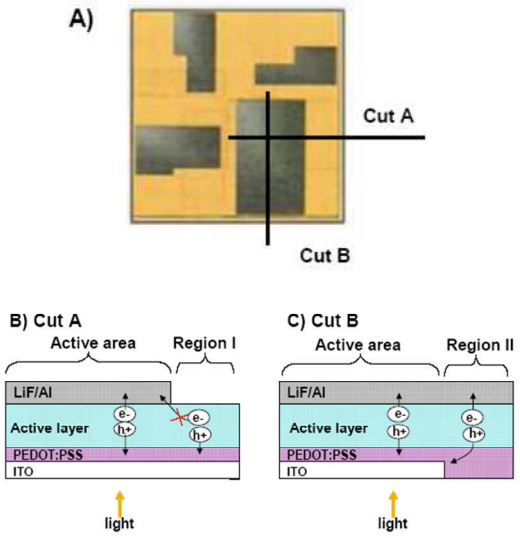

Figure 9: A) Device lay out top view. B) Side view for cut along line A. C) Side view for cut along line B.

In Region I the photogenerated electrons cannot be collected by the metal electrode due to the low conductivity of the active layer. In Region II the photogenerated holes can be collected by the highly conductive PEDOT layer. The contribution of this region to the photocurrent should be prevented. The determination of the additional active area is difficult. Thus the use of an illumination mask can prevent the contribution of Region II and is an easy to implement technique.

P3HT:PCBM devices on standard and on neutral PEDOT have been measured with and without an illumination mask. The EQE measurements are shown in Fig. 10.

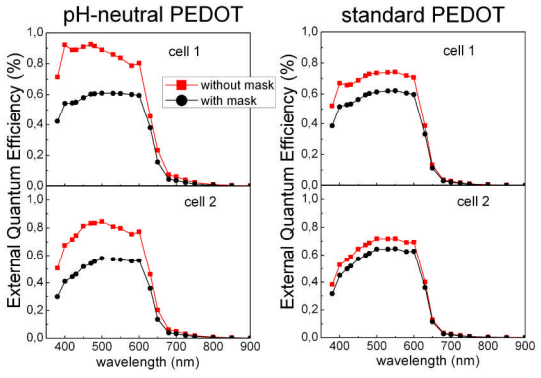

Figure 10: EQE recorded with and without illumination mask for P3HT:PCBM devices on pH-neutral and standard PEDOT. Devices with different areas (cell 1 = 0.093 cm^2 and cell 2 = 0.164 cm^2) are also compared.

The use of a mask can result in a measured current density which is 10-40% (depending on cell area and the type of PEDOT employed) lower than the current density measured without a mask. The region outside the active area can thus be considered as a parasitic contribution.

Besides the overestimation in current density, the fill factor is also influenced by the parasitic contribution of Region II. We observe higher fill factors when an illumination mask is used, as shown in Fig. 11. The real and parasitic solar cells are connected in parallel and the low fill factor of the parasitic solar cell lowers the overall fill factor.

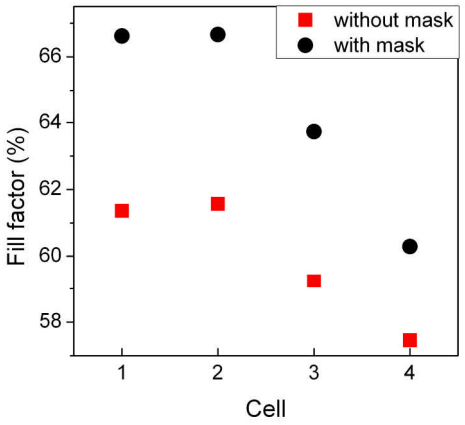

Figure 11: Fill factor of four P3HT:PCBM devices (cell 1, 2, 3, 4 have an active area of 0.093, 0.164, 0.364 and 1.003 cm^2 respectively) on standard PEDOT.

3.4.2 Spectral Response (SR)

To measure accurate cell efficiencies it is necessary to determine the mismatch factor of the multi-junction device. For this mismatch factor, spectral response measurements of the individual subcells are necessary. In order to measure the spectral response for each sub cell in a series connection, the sub cell under investigation must be current limiting [15]. This can be achieved by saturating the other sub cell with a bias light. This bias light must have a wavelength that is strongly absorbed by the cell to be biased, and not absorbed by the cell under investigation. In our home built set-up, the bias light can be applied by either a ring of 20 LED lights, or by a halogen lamp with filters. The set-up was tested on a microcrystalline Si/amorphous Si tandem, as described in ref [16].

For the mechanical stack described in Fig. 2, it is possible to successfully bias the MDMO-PPV:PCBM cell and measure the SR of the PF10TBT:PCBM cell. The PF10TBT:PCBM cell is already the current limiting cell almost over the whole spectral range as shown by the dark measurement in Fig. 12. When using LED bias illumination at 470 nm, the SR of the bottom cell of the stack in the two-terminal measurement is almost identical to the output of the bottom cell in the four-terminal situation as can be seen in Fig. 12. Alternatively, a halogen lamp in combination with a bandpass filter was applied as bias light source. The result is presented in Fig. 12, showing that this type of illumination is also able to measure the correct SR of the bottom cell. Thus, both the LED illumination, as well as the halogen lamp with filter illumination, result in a correct SR measurement

However, biasing the PF10TBT:PCBM cell without generating current in the MDMO-PPV:PCBM cell is difficult due to the overlap in the spectral response. A narrow, yet sufficiently intense light beam is needed for this bias.

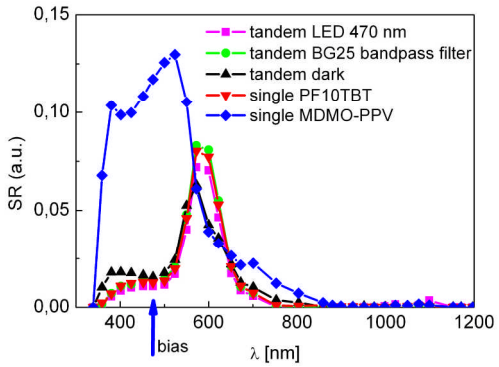

Figure 12: Spectral response of the bottom PF10TBT:PCBM cell in the mechanically stacked tandem cell, measured by applying a bias light with LEDs at 470 nm to the top MDMO-PPV cells.

When bias light is applied to one of the sub cells, this cell will be close to its V_{oc} value. The other sub cell will consequently not be at zero volt, but close to $-V_{oc}$. Due to the relatively low fill factor of polymer solar cells, the measured current at $-V_{oc}$ is larger than at 0 V (see e.g. Fig. 7), resulting in an overestimation of the current. Therefore, it is also necessary to apply a bias voltage [17] to the multi-junction structure when measuring the (absolute) SR.
For correct characterization of the multi-junction structures we are further adapting the spectral response set-up with suitable bias light, as the polymer layer require narrow bandwidth bias light. The incorporation of bias voltage is also needed in order not to overestimate the measured current density.

4 CONCLUSIONS AND OUTLOOK

We have reported on the successful synthesis of a monolithic polymer-based tandem cell fabricated by solution processing and containing a ZnO/pH-neutral PEDOT recombination layer. The use of pH-neutral PEDOT results in a lower V_{oc} than the use of standard PEDOT and the voltage drop is largest in PF10TBT:PCBM devices (0.3 V). The use of an optical mask is necessary in order to avoid an overestimation of the current density, which can be between 10-40%. In order to measure the spectral response of multi-junction cells, narrow and intense bias light is needed, as well as bias voltage.
TiOx layers are expected to be more robust than ZnO layers because TiOx is chemically less reactive and does not dissolve in acidic solutions. Furthermore, processing from a precursor solution is likely to result in closed layers, whereas the ZnO processed from nanoparticle solution will be partially porous. In this work, we presented a strongly reduced current density for polymer solar cells with a TiOx layer compared to cells without a TiOx layer. Different synthesis routes, such as via a TiOx precursor solution without ethanolamine and methoxy-ethanol, and under controlled atmosphere offer possibilities. The workfunction might also have an influence on the current density as a wrong workfunction might result in blocking electrodes. This must be investigated.

Different device geometries offer an opportunity to increase the window of available materials for multi-junction fabrication, both in terms of substrate employed and in terms of suitable anode and cathode materials.

The efficiency of the multi-junction reported here is lower than for a single junction of the same material [18]. We calculated that for a tandem structure using two layers of PF10TBT, the maximum gain in efficiency compared to a single junction is 20%, if FF and V_{oc} remain the same [10]. Significant increase in efficiency can only occur for multi-junctions with different materials that have a complementary optical absorption [19]. The synthesis of novel, low band-gap materials is currently an important issue and has resulted in 2 promising candidates. Indeed an efficiency around 6.5% has been reported for a tandem structure containing a low bandgap polymer (PCPDTBT) and P3HT [8]. Combining the low band gap polymer with the PF10TBT reported here would offer a very interesting multi-junction structure.

5 ACKNOWLEDGEMENTS

We thank J. Sweelsen and M. M. Koetse from TNO Eindhoven, The Netherlands, for supplying the PF10TBT polymer. We thank T. Söderström from the University of Neuchâtel (Institute of Microtechnology), Neuchâtel, Switzerland) for kindly supplying a micro-crystalline/amorphous Si tandem cell, which has been used to test the modified spectral response set-up. We further thank J. Gilot, M. M. Wienk and R.A.J. Janssen from the Eindhoven University of Technology, Eindhoven, The Netherlands, for supplying the pH neutral PEDOT.
This work has been supported by the Senter/Novem, The Netherlands in the EOS project Zomer (EOSLT03026).

7 REFERENCES

[1] M. Green *et al.*, Prog. Photovolt: Res. Appl. 16 (2008) 435.
[2] R. Kroon *et al.*, Polymer Reviews 48 (2008) 531.
[3] M. C. Scharber *et al.*, Adv. Mater. 18 (2006) 789.
[4] L. J. A. Koster *et al.*, Appl. Phys. Lett. 88 (2006) 093511.
[5] J. Peet *et al.*, Nature Materials 6 (2007) 497.
[6] M. Wienk *et al.*, Adv. Mater. 20 (2008) 2556.
[7] J. Gilot *et al.*, Appl. Phys. Lett. 90 (2007) 143512
[8] J.Y. Kim *et al.*, Science 317 (2007) 222.
[9] N.K. Persson, H. Arwin, O. Iganäs, J. Appl. Phys. 97 (2005) 034503.
[10] W. Eerenstein, L.H. Slooff, S.C. Veenstra, J.M. Kroon, Thin Sol. Films 516 (2008) 7188.
[11] V. Shrotriya, E.H.E. Wu, G. Li, Y. Yao, Y. Yang, Appl. Phys. Lett. 88 (2006) 064104.
[12] M.M. De Kok et al., Physica status solida a 201 (2004) 1342.
[13] A.Cravino, P.Schilinsky, J.C.Brabec, Avd. Funct. Mater. 17 (2007) 3906.
[14] M.S.Kim, M.G.Kang, L.J.Guo and J.Kim, Appl. Phys. Lett. 92 (2008) 133301.
[15] J. Burdick and T. Glatfelter, Solar Cells 18 (1986) 301.
[16] L.H. Slooff *et al.*, Proceedings SPIE Optics &

Photonics Conference 2008, submitted for publication.
[17] K. Büchner and A. Schönecker, Proceedings 10th European Photovoltaic Solar Energy Conference, Vol. I (1991) p 107.
[18] L.H. Slooff *et al.*, Appl. Phys. Lett. 90 (2007) 143506.
[19] G. Dennler *et al.*, J. Appl. Phys. 102 (2007) 123109.